^{30}Si(^{3}He,d)^{31}P reaction at 25 MeV

J. Vernotte, A. Khendriche,* G. Berrier-Ronsin, S. Grafeuille, J. Kalifa, and G. Rotbard
Institut de Physique Nucleáire, B.P.1, 91406 Orsay CEDEX, France

R. Tamisier
Institut de Physique Nucleáire, B.P.1, 91406 Orsay CEDEX, France
and Laboratoire de Physique de Nantes, 2 rue de la Houssinière, 44072 Nantes CEDEX 03, France

B. H. Wildenthal
Department of Physics and Astronomy, University of New Mexico, 800 Yale NE, Albuquerque, New Mexico 87131
(Received 12 April 1989)

The ^{30}Si(^{3}He,d)^{31}P reaction has been investigated at 25 MeV incident energy. About 80 levels were observed up to an excitation energy of 10 MeV by using a split-pole magnetic spectrograph. Most of the proton-unbound states were identified with resonance levels observed in proton capture reactions on ^{30}Si. Four levels were observed for the first time in a reaction which couples a proton to a ^{30}Si core. Spectroscopic information has been obtained for about 60 levels through angular distribution measurements and distorted wave Born approximation analyses, with special treatment applied in the cases of the proton-unbound states. The spectroscopic factors of the proton-unbound states are in overall agreement with the spectroscopic factors which are deduced from the proton partial widths measured in resonant proton scattering experiments, but the proton partial width which is obtained in this work for the 7897 keV level is in disagreement with previous values from γ-ray resonant absorption measurements. The strengths of the $l=0$, 2, and 3 transfers are essentially concentrated into one level, each of isospin $T=\frac{1}{2}$ and $T=\frac{3}{2}$. In contrast the $l=1, T=\frac{1}{2}$, strength is distributed over many levels, especially in a cluster of six levels between 9.0 and 9.8 MeV. The sum rule for the $2p_{3/2}, T=\frac{1}{2}$, proton single-particle strength is exhausted, leading to a centroid energy of about 7.9 MeV for this configuration. Isospin assignments are discussed for some levels. The excitation energies and spectroscopic factors for even-parity states are compared with the results of a recent, complete *sd*-shell space, shell-model calculation.

I. INTRODUCTION

During the last twenty years, states in ^{31}P have been investigated several times by means of single-proton stripping reactions on a ^{30}Si target. Levels up to 7.2 MeV were observed in the studies of the (^{3}He,d) reaction which were carried out at incident energies of 12 MeV,[1] 15 MeV,[2] and 18 MeV.[3] More recently, a study of the same reaction at 33 MeV using a polarized beam[4] was limited to seven strongly populated levels (including a level at 9.4 MeV). Additionally, ^{31}P states were studied up to 8.6 MeV excitation energy through the (d,n) reaction[5] at 7 MeV. Comparison of the spectroscopic factors extracted from these studies with the sum rules of French and Macfarlane[6] indicates that most of the existing $l=0$ and $l=2$ proton strength is concentrated into the levels observed in these works, but a large part of the $l=1$ and $l=3$ strengths does not appear in the range of excitation energy below 8 MeV. Therefore, the levels which carry the bulk of the $l=1$ and $l=3$ proton transfer strength should lie at higher excitation energies. In fact, many $l=1$ levels have been observed at excitation energies lying between 9 and 10 MeV in a study of the ^{30}Si(p,p)^{30}Si reaction[7] done with an overall energy resolution of 350–450 eV.

The principal motivation for this new study of the ^{30}Si(^{3}He,d)^{31}P reaction was to measure the amount of $l=1$ strength concentrated in these levels. An additional motivation for reinvestigating the $l=0$ and $l=2$ transitions was the need for more accurate experimental values of spectroscopic factors with which to test the latest generation of shell-model wave functions for *sd*-shell nuclei. A critically important aspect of these model calculations is the relative occupancies of the three *sd*-shell orbits near the middle of the shell. The position of ^{31}P in the shell makes it an essential component of such a test of the model results.

This study was performed at an incident energy of 25 MeV and covered an excitation energy range of about 10 MeV. The incident energy is optimum for (^{3}He,d) studies. At 25 MeV the matching conditions favor $l=2$ transfers for levels located between 7 and 10 MeV excitation energy, so $l=1$ and $l=3$ transfers should be optimally populated in the same excitation energy range.

II. EXPERIMENTAL PROCEDURE

A 25 MeV ^{3}He beam from the Orsay MP Tandem Van de Graaff accelerator was focused onto a self-supporting target, 73 ± 4 μg cm^{-2} thick, which was prepared by eva-

poration in vacuum of enriched metallic silicon (95% ^{30}Si). This target is placed at the center of a scattering chamber. The beam was then stopped in a graphite Faraday cup connected to a current integrator. The target thickness was deduced from the measurement at three angles ($\theta_{lab}=24°$, 27°, and 30°) of the 25 MeV ^{3}He elastic scattering. The cross section of this reaction has been previously measured at this energy[8] with an accuracy of 5% in a wide angular range which included these three angles. A noticeable amount of oxygen was present in the target. A surface barrier detector, mounted inside the scattering chamber at $\theta_{lab}=42°$ with respect to the beam direction, was used as a monitor during the angular distribution measurements.

Deuterons were momentum analyzed with an Enge split-pole magnetic spectrograph and detected with a combination of three counters located in the focal plane. The first of these counters is a 50 cm long position-sensitive proportional counter similar to the one described in Ref. 9. The second one is a proportional counter acting as a ΔE detector. The third counter is a plastic scintillator which gives a light-output signal proportional to the amount of energy deposited in the plastic by the detected particle. The signals from the three counters were stored on a magnetic tape after processing by a SOLAR 16-40 computer.

The horizontal entrance aperture of the spectrograph was set to $\pm 1°$, which yielded a solid angle of $\Omega \simeq 1.1$ msr. The angular distributions were obtained by taking spectra at 13 angles: $\theta_{lab}=5°$, 8°, 10°, 12°, 14°, 17°, 20°, 25°, 30°, 35°, 40°, 45°, and 50°. The total charge ($Q_{^{3}He^{++}}$) accumulated during the measurements ranged from 125 μC at $\theta_{lab}=5°$ up to 800 μC at $\theta_{lab}=50°$. The beam intensity was restricted to 100 nA for the two forward angles in order to keep the counter dead time to less than 5%. The deuteron spectrum measured at $\theta_{lab}=5°$ is displayed on Fig. 1. In addition to the peaks which correspond to (^{3}He,d) reactions on ^{30}Si and ^{16}O nuclei, other peaks are observed which can be attributed to the (^{3}He,d) reaction on the ^{12}C, ^{28}Si, and ^{29}Si contaminations present in the target. The weak ^{12}C contamination is attributed to carbon buildup on the self-supported target. The full width at half maximum of the deuteron peaks was about 23 keV for all the peaks with negligible natural widths. This experimental width is due mainly to the target thickness.

III. ANALYSIS OF SPECTRA AND EXCITATION ENERGIES ASSIGNMENTS

In order to get peak positions and integrated counts in the individual peaks, the reaction spectra were analyzed with the multipeak fitting code PICOTO,[10] a modified ver-

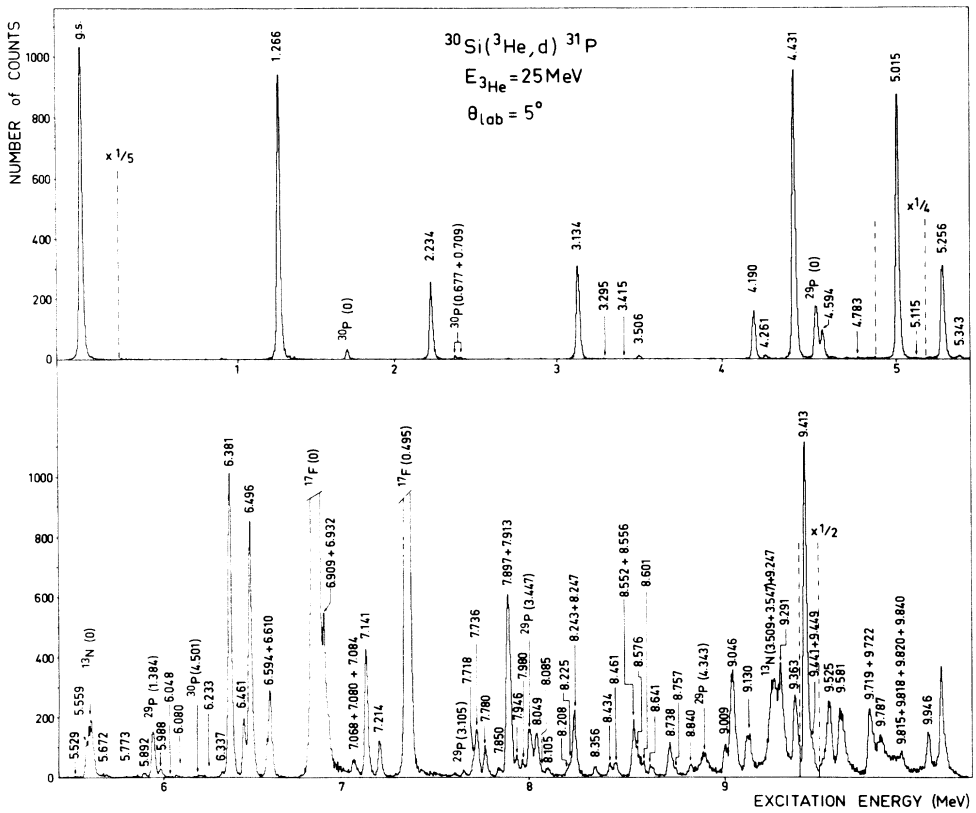

FIG. 1. Spectrum of the ^{30}Si(^{3}He,d)^{31}P reaction at $\theta_{lab}=5°$. The excitation energies are from Ref. 12 for $E_x < 9.7$ MeV and from Ref. 7 for $E_x > 9.7$ MeV. As for the peaks at 9.13 and 9.25 MeV, see text, Sec. IV. The last peak near 10 MeV excitation energy is due to the effect of the counter edge.

sion of the code AUTOFIT (Ref. 11) adapted to the VAX 85-30 computer of the Institute. Peaks which appear at excitation energies higher than 9.5 MeV can correspond to the population of states which have natural widths of several keV's.[12] Since choosing a standard shape for the analysis of these peaks is difficult, the simpler computer code HYPOGRAF, which yields the centroids and the integrated counts for any group of counts between two channels, was used for them instead of the code PICOTO.

Absolute cross sections were obtained from the summed counts for each peak by normalization to the 25 MeV ^{3}He scattering data obtained with the same target at three forward angles (see Sec. II). The quoted accuracy of the reaction cross-section values was obtained by combining the errors of the normalization procedure (5%) with the one arising from the statistics.

Excitation energies were derived from the peak positions by using a relationship between the radius of curvature of the deuteron in the spectrograph and the corresponding peak position in the counter. This relationship was obtained by considering ten peaks which are strongly populated at $\theta_{lab}=8°$ in the ^{31}P(^{3}He,d)^{32}S reaction which has been studied previously[13] at the same energy of 25 MeV. Spectra from this reaction were obtained for five different adjustments of the magnetic field in the spectrograph in order to extend the range of validity of the relationship to the total length of the counter. Using this procedure the excitation energies were obtained with an accuracy of ±4 keV for 75 levels (or groups of levels) up to 9.7 MeV. They are presented and compared with the more accurate values from Ref. 12 in Table I. The latter values were adopted in the following parts of this paper whenever the agreement between the present values and those of Ref. 12 is good.

The widths of some peaks are larger than the 23 keV instrumental resolution even at excitation energies below

TABLE I. Comparison of present results with previously existing information on ^{31}P levels below $E_x=10$ MeV.

This work			Other values of C^2S (^{3}He,d)				(d,n)	Excitation energy and $(J^\pi;T)$ assignments[a]			New J^π
E_x (keV) ±4 keV	l_p	C^2S[b]	c	d	e	f	g	E_x (keV)	E_p (keV)	$J^\pi;T$	assignment (This work)
0	0	0.64	0.47	0.44	0.49	0.34	0.53	0		$\frac{1}{2}^+$	
1268	2	0.69	0.48	0.80	0.65	0.36	0.56	1266.2±0.1		$\frac{3}{2}^+$	
2227	2	0.06	0.05	0.08	0.08	0.05	0.04	2233.7±0.2		$\frac{5}{2}^+$	
3134	0	0.03	0.02	0.03	0.03		0.01	3134.1±0.3		$\frac{1}{2}^+$	
3297	(2)	<0.001	<0.01	<0.01				3295.0±0.2		$\frac{5}{2}^+$	
3414								3414.6±0.3		$\frac{7}{2}^+$	
3501	(2)	0.006	<0.01	<0.01				3505.8±0.5		$\frac{3}{2}^+$	
4189	2	0.03	0.02	0.02				4190.3±0.4		$\frac{5}{2}^+$	
4258	2	0.005	0.01		0.06			4260.7±0.7		$\frac{3}{2}^+$	
4429	3	0.30	0.34	0.29	0.36	0.24	0.26	4430.9±0.3		$\frac{7}{2}^-$	
4590	2	0.03	0.02	0.03	0.06			4593.6±0.8		$\frac{3}{2}^+$	
								4633.8±0.5		$\frac{7}{2}^+$	
4789	(2)	<0.001	<0.01					4783.1±0.5		$\frac{5}{2}^+$	
5013	1	0.17	0.17	0.21	0.24	0.16	0.15	5014.9±1.0		$\frac{3}{2}^-$	$\frac{3}{2}^-$
								5015.2±0.8		$\frac{1}{2}(\frac{3}{2}^+)$	
5112	(2)	<0.001						5115.4±0.6		$\frac{5}{2}^+$	
5255	0	0.05	0.03	0.07	0.05		0.02	5256.1±1.4		$\frac{1}{2}^+$	
5345								5343.1±0.5		$\frac{9}{2}^+$	
5525								5529.3±0.8		$\frac{7}{2}^+(\frac{5}{2}^+)$	
5560	2	0.02	0.02					5559.2±1.1		$\frac{3}{2}^+$	
5674								5672.3±0.9		$\frac{5}{2}$	
5775								5773.1±0.8		$(\frac{5}{2},\frac{7}{2}^+)$	
5892								5892.3±0.6		$\frac{9}{2}^+$	
5988	2	0.007						5987.9±1.2		$\frac{3}{2}^-$	$(\frac{3}{2},\frac{5}{2})^+$
6051								6047.8±1.0		$\frac{7}{2}^+$	
6080								6080.1±1.4		$\frac{9}{2}^+$	
6234								6233.1±1.3		$(\frac{3}{2}^+,\frac{9}{2}^+)$	
6336	0	0.004						6336.6±1.5		$\frac{1}{2}^+$	
6381	2	0.22	0.18	0.25	0.25	0.33	0.12	6380.8±1.7		$\frac{3}{2}^+;\frac{3}{2}$	
								6398.6±0.7		$(\frac{5}{2}^-,\frac{7}{2})$	
								6453.7±1.1		$\frac{11}{2}^+$	
6462	2	0.04	0.03					6460.8±1.6		$(\frac{3}{2},\frac{5}{2})^+$	
6496	1	0.05	0.05	0.14	0.07		0.03	6495.8±1.2		$(\frac{1}{2},\frac{3}{2})^-$	

Table I. (*Continued*).

This work			Other values of C^2S (^{3}He,d)				(d,n)	Excitation energy and $(J^\pi;T)$ assignments[a]			New J^π
E_x (keV) ±4 keV	l_p	C^2S[b]	c	d	e	f	g	E_x (keV)	E_p (keV)	$J^\pi;T$	assignment (This work)
								6500.6±0.9		$\frac{9}{2}^-$	
6594	3	0.03	0.02				0.04	6594.2±1.4		$\frac{5}{2}^-$	
6610	1	0.02	0.02	0.01	0.04		0.01	6610.3±1.0		$\frac{3}{2}^-$	
6797								6792.9±0.9		$\frac{9}{2}^-$	
6826								6825.1±0.9		$\frac{11}{2}^-$	
6843	3	0.005	0.01					6842.3±1.2		$(\frac{5}{2},\frac{7}{2})^-$	
6910	1	0.02	0.02	0.07			0.02	6909.2±1.4		$\frac{3}{2}^-$	
6932	2	0.02	0.01					6931.7±1.4		$\frac{5}{2}^+$	
7068	3	0.005									$(\frac{5}{2},\frac{7}{2})^-$
7081								7079.9±1.9		$(\frac{3}{2}^-,\frac{5}{2}^+)$	
								7084.0±1.7		$(\frac{3}{2}^+,\frac{7}{2}^+)$	
								7117.9±0.7		$\frac{9}{2}^{(+)}$	
7139	0	0.11	0.08	0.08	0.34		0.04	7140.6±1.5		$\frac{1}{2}^+;\frac{3}{2}$	
7214	1	0.008	0.01					7214±2		$(\frac{1}{2},\frac{3}{2})^-$	
7314	3	0.002						7313.7±1.6		$(\frac{1}{2},\frac{5}{2}^+)$	$(\frac{5}{2},\frac{7}{2})^-$
								(7356±9)			
								7441.2±0.7		$\frac{11}{2}^+$	
								7466±2		$(\frac{7}{2}^-,\frac{9}{2})$	
								(7687±2)			
7718								7718±9			
7736	3	0.02									$(\frac{5}{2},\frac{7}{2})^-$
7780	1	0.005						7779.5±1.2	498.9±1.0	$\frac{3}{2}^-$	
								7825±12			
7855								7850±4		$(\frac{1}{2},\frac{5}{2}^+)$	
7900	1	0.08					0.11	7897.0±1.4	620.4±1.2	$\frac{1}{2}^-$	
7913	3	0.03									$(\frac{5}{2},\frac{7}{2})^-$
7949	2	0.01						7945.7±1.2	670.7±1.0	$\frac{3}{2}$	$\frac{3}{2}^+$
	2	0.008									$(\frac{3}{2},\frac{5}{2})^+$
7980	or										
	3	0.004									$(\frac{5}{2},\frac{7}{2})^-$
								8032.4±1.1	760.3±0.9	$\frac{5}{2};(\frac{3}{2})$	
8051	1	0.01					0.01	8048.9±1.2	777.4±1.0	$\frac{3}{2}^-$	
8080								(8085±11)			
8107	2	0.003						8104.9±1.5	835.3±1.3	$\frac{5}{2};(\frac{3}{2})$	$\frac{5}{2}^+$
8209								8208.2±0.9	942.0±0.6	$\frac{3}{2}$	
8227								8224.9±0.9	959.3±0.6	$\frac{7}{2}$	
8246	1+3	(0.02)						8243.2±0.9	978.2±0.6	$\frac{5}{2}^-$	
		(0.01)						8247.3±0.9	982.5±0.6	$\frac{3}{2}^-$	
								8345.5±1.5		$(\frac{7}{2}^-,\frac{9}{2}^+)$	
8355	3	0.006						8355.8±0.9	1094.6±0.6	$\frac{5}{2}$	$\frac{5}{2}^-$
8433	3	0.005						8434.0±1.0	1175.4±0.7	$\frac{7}{2}$	$\frac{7}{2}^-$
8462	2	0.004						8461.1±1.0	1203.4±0.7	$\frac{5}{2}^+$	
								8470.4±1.0	1213.1±0.7	$\frac{5}{2}$	
								8543.7±1.1	1288.8±0.8	$\frac{1}{2}^-$	
8553	0+	(0.02)						8552.3±1.1	1297.7±0.8	$\frac{1}{2}^+$	
		(0.01)					0.02	8555.5±1.1	1301.0±0.8	$\frac{3}{2}^-$	
8574								8575.7±1.1	1321.9±0.8	$\frac{5}{2}^+$	
								8584.2±1.1	1330.7±0.8	$\frac{1}{2}^-$	
8600								8601.0±1.1	1348.1±0.8	$\frac{5}{2}^+$	
8642	2	0.004						8641.3±1.1	1389.7±0.8	$\frac{5}{2}^+$	
								8649.5±1.1	1398.2±0.8	$\frac{3}{2}^{(+)}$	

Table I. (*Continued*).

This work			Other values of C^2S (^{3}He,d)				(d,n)	Excitation energy and $(J^\pi;T)$ assignments[a]			New J^π
E_x (keV) ±4 keV	l_p	C^2S[b]	c	d	e	f	g	E_x (keV)	E_p (keV)	$J^\pi;T$	assignment (This work)
								8729.1±1.1	1480.5±0.8	$\frac{3}{2}^{(+)}$	
								8730.6±1.1	1482.0±0.8	$\frac{3}{2}$	
8735	2	0.02						8738.0±1.1	1489.7±0.8	$\frac{3}{2}^+;\frac{3}{2}$	
								8754.3±1.1	1506.5±0.8		
8758								8757.4±1.1	1509.7±0.8	$\frac{5}{2}^+$	
								8763.4±1.1	1515.9±0.9	$\frac{1}{2}^+$	
8840	2	0.004						8840.0±1.1	1595.1±0.9	$\frac{7}{2}^-$	
								8903.0±1.2	1660.2±1.0	$\frac{1}{2}^+$	
								8909.8±1.2	1667.2±1.0	$\frac{5}{2}^+$	
								8935.9±1.2	1694.2±1.0	$\frac{3}{2}^+$	
								8985.9±1.2	1745.9±1.0	$\frac{3}{2}$	
9015	2	0.008						9009.1±1.3	1769.9±1.1	$\frac{5}{2}^+;(\frac{3}{2})$	
9052	1	0.07						9046.2±1.3	1808.2±1.1	$\frac{3}{2}^-$	
								9052.8±1.3	1815.0±1.1	$(\frac{3}{2}^+,\frac{5}{2})$	
								9067.2±1.3	1829.9±1.1	$\frac{5}{2}^+;(\frac{3}{2})$	
8246	1+3							9113.6±0.9	1877.9±0.6	$\frac{7}{2}^-$	
								9115.7±0.9	1880.1±0.6	$\frac{5}{2}^+;(\frac{3}{2})$	
9130								9128.7±0.9	1893.5±0.6	$\frac{5}{2}^+;(\frac{3}{2})$	
								9131.1±0.9	1896.0±0.6	$\frac{5}{2}^+;(\frac{3}{2})$	
								9154.4±0.9	1920.1±0.6	$\frac{7}{2}$	
								9156.5±0.9	1922.2±0.6	$\frac{3}{2}^{(+)}$	
								9176.2±0.9	1942.6±0.6	$\frac{3}{2}^-$	
								9206.3±0.9	1973.7±0.6	$\frac{7}{2}$	
								9226.5±0.9	1994.6±0.6	$\frac{1}{2}^-$	
9247								9240.9±0.9	2009.5±0.7	$\frac{3}{2}^+$	
								9253.1±1.0	2022.1±0.7	$\frac{7}{2}^-$	
								9256.1±1.0	2025.2±0.7	$\frac{7}{2}$	
9294	1	0.04						9291.0±1.0	2061.3±0.7	$\frac{3}{2}^-$	
								9319.8±1.1	2091.0±0.8	$\frac{1}{2}$	
								9358.4±1.1	2130.9±0.8	$(\frac{7}{2})$	
								9361.1±1.1	2133.7±0.8	$(\frac{7}{2})$	
9360	1	0.05						9362.6±1.1	2135.3±0.8	$\frac{3}{2}^-$	
								9400.0±1.1	2173.9±0.8	$\frac{1}{2}^+$	
9410	3	0.21				0.20		9412.7±1.1	2187.0±0.8	$\frac{7}{2}^-;(\frac{3}{2})$	
9447	2	0.02[h]						9441.0±1.1	2216.3±0.9	$\frac{3}{2}^+$	
								9449.1±1.1	2224.7±0.9	$\frac{5}{2}^+$	
								9477.2±1.1	2253.7±0.9	$\frac{7}{2}^-$	
9522	1	0.07						9524.9±1.1	2303.0±0.9	$\frac{3}{2}^-$	
								9536.7±1.2	2315.2±1.0	$(\frac{3}{2},\frac{5}{2})^+$	
								9570.7±1.2	2350.4±1.0	$\frac{3}{2}$	
								9578.0±1.2	2357.9±1.0	$(\frac{3}{2},\frac{5}{2})^+$	
9577	1	0.07						9580.7±1.2	2360.7±1.0	$\frac{3}{2}^-$	
								9585.3±1.2	2365.4±1.0	$\frac{1}{2}^+$	
								9594.1±1.2	2374.5±1.0		
								9598.7±1.2	2379.3±1.0		
								9612.1±1.2	2393.2±1.0		
9720	1+3	(0.02)	for $l=3$					9719±3	2503±3	$(\frac{5}{2},\frac{7}{2})^-$	
		(0.03)	for $l=1$					9722±3	2506±3	$\frac{3}{2}^-$	
9800	1	0.07						9787±3	2574±3	$\frac{3}{2}^-;(\frac{3}{2})$	

Table I. (*Continued*).

This work			Other values of C^2S					Excitation energy and $(J^\pi;T)$ assignments[a]			New J^π
E_x (keV) ±4 keV	l_p	C^2S[b]	(^{3}He,d) c	d	e	f	(d,n) g	E_x (keV)	E_p (keV)	$J^\pi;T$	assignment (This work)
								9815±3	2603±3	$(\frac{5}{2},\frac{7}{2})^-$	
9830	1+3	(0.007)	for $l=3$					9818±3	2605±3	$\frac{3}{2}^-$	
		(0.03)	for $l=1$					9820±3	2608±3	$\frac{3}{2}^-$	
								9840±3	2628±3	$(\frac{7}{2}^-)$	
9950	3	0.01						9946±3	2738±3	$(\frac{5}{2})^-$	

[a]Reference 12 for $E_x<9.7$ MeV and Ref. 7 for $E_x>9.7$ MeV. In the latter case, only the levels which can contribute to the population of the four peaks observed in the present work are presented in the table.

[b]$E_{^3\mathrm{He}}=25$ MeV; for a level with a not uniquely determined J^π value, the proton transfer is assumed to be $2p_{3/2}$, $1d_{3/2}$, and $1f_{7/2}$ for transitions $l=1$, 2, and 3, respectively. The relationship $C^2S(j=l-\frac{1}{2})\approx 2C^2S(j=l+\frac{1}{2})$ can be considered as correct.

[c]$E_{^3\mathrm{He}}=12$ MeV (Ref. 1).

[d]$E_{^3\mathrm{He}}=15$ MeV (Ref. 2).

[e]$E_{^3\mathrm{He}}=18$ MeV (Ref. 3).

[f]$E_{^3\mathrm{He}}=33$ MeV (Ref. 4).

[g]$E_d=7$ MeV (Ref. 5).

[h]With consideration of the measured proton partial widths of Ref. 7, the $J^\pi=\frac{5}{2}^+$ member of this unresolved doublet is expected to be more strongly populated than the $J^\pi=\frac{3}{2}^+$ one. So, the C^2S value was extracted with the assumption of $J^\pi=\frac{5}{2}^+$.

the particle-emission threshold. For instance, this is the case for the peak which appears at 6.6 MeV in Fig. 1. This larger width is thought to correspond to the simultaneous population of two or more levels occurring at nearly the same excitation energy, since a large natural width is not expected for an isolated level at this excitation energy. Indeed, two levels are known to lie around this energy,[12] at 6594 and 6610 keV. This peak was therefore taken as an example with which to test the capability of the multipeak fitting procedure to decompose an unresolved superposition of two peaks. Special attention was paid to the analysis by verifying that the final result is not dependent upon the initial peak position values introduced in the code PICOTO. Thus it has been found that the peak at 6.6 MeV corresponds to the population of two levels, at 6594 and 6610 keV, as had been observed in previous single-proton transfer reactions.[1,5]

Above 7297 keV the states of ^{31}P are proton unbound. Most of these proton-unbound states are identified in Table I with states previously observed in the resonance proton capture reactions on a ^{30}Si target. Some special points will be discussed in Sec. V A. Several of these resonance levels are too closely spaced to be experimentally resolved in this work, and they appear as single peaks in the deuteron spectra if they are populated in the stripping reaction. The same precautions as indicated above were taken for the analysis of these peaks with the code PICOTO. When the presence of at least two levels populated with different intensities is suggested by the asymmetrical shape of a peak, it was found that for the more intense component, the peak position and the integrated counts are little changed when the initial values of the fitting procedure are changed, while for the less intense component the peak position is again little changed, but the integrated counts are much more affected. Therefore, the excitation energy of the weak component can be obtained from the peak position, but the extraction of the integrated counts is too uncertain to yield reliable angular distributions.

For the peaks at 9130 and 9247 keV the results obtained with the code PICOTO are not independent of the initial values of the fitting procedure, so the excitation energies were calculated from the centroids obtained with the code HYPOGRAF.

The excitation energies of four peaks which appear above 9.7 MeV are also presented in Table I. The errors in the energies are estimated to be ±15 keV. This increase in the assigned error is due to effects of the counter edge which produced perturbations in the energy calibration curve. The identification of these peaks with levels or groups of levels which are already known from Refs. 7 and 12 will be attempted in the next section by using the results of the angular distribution analyses.

IV. ANGULAR DISTRIBUTION ANALYSES

The measured angular distributions are compared with the results of DWBA calculations done with the code DWUCK4 (Ref. 14) in the local, zero-range approximation. In the case of a doubly even target nucleus, such as ^{30}Si, the spectroscopic factors are obtained from the relationship

$$\left[\frac{d\sigma(\theta)}{d\omega}\right]_{\mathrm{exp}}=4.43C^2S_{lj}\left[\frac{d\sigma_{lj}(\theta)}{d\omega}\right]_{\mathrm{DWUCK4}},$$

where 4.43 is the commonly used normalization factor for the (^{3}He,d) reaction[15] and S_{lj} is the spectroscopic factor for an orbital momentum l and total angular momentum j transfer. The isospin Clebsch-Gordan coefficients C^2 are equal to $\frac{2}{3}$ and $\frac{1}{3}$ for the $T=\frac{1}{2}$ and $T=\frac{3}{2}$ states, respectively.

Finite-range and nonlocality corrections were investigated and found to result in a factor of 0.77 reduction in

extracted spectroscopic factors. The l and Q dependences of this reduction factor were found to be less than 3% for the range of states studied. The nonlocal parameters for ^{3}He, deuteron, and proton were 0.25 fm, 0.54 fm, and 0.85 fm, respectively. The finite-range parameter was 0.77 fm.[15] The radius of the potential for the proton form factor, a parameter which correlates strongly with the magnitude scale of the extracted spectroscopic factors, was set to $r_0=1.25$ fm. The optical model parameters used for all of these calculations are presented in Table III. The deuteron parameters are taken from Ref. 16 (L potential) and the ^{3}He parameters are taken from a systematic study of the ^{3}He elastic scattering on many s-d shell nuclei.[8] In selecting the ^{3}He parameters, three sets from Ref. 8 were considered, with real depths V_r equal to about 80 MeV, 130 MeV, and 180 MeV, respectively. These ^{3}He sets were used in conjunction with the deuteron potential and the results for (^{3}He,d) angular distributions compared with experimental distributions for some strongly excited states, namely the ground state ($l=0$), and the 5015 keV ($l=1$), 1266 and 6381 keV ($l=2$), and 4431 keV ($l=3$) states. The $V_r\simeq 80$ MeV set was rejected after this comparison because its predictions failed to fit the observed $l=0$ transition. The other two sets lead to almost equal C^2S values, but the backward-angle experimental points are better accounted for by the deepest potential. This "deep" potential was therefore adopted. A similar choice of a deep ^{3}He optical potential was also made in a previous study, at the same energy, of the ^{31}P(^{3}He,d)^{32}S reaction.[13]

The proton bound-state form factor was computed with a standard Woods-Saxon well, the depth of which was adjusted to reproduce the experimental proton separation energy. For the proton-unbound states, the spectroscopic factors were obtained by means of a procedure of Vincent and Fortune.[17] This procedure is included in the 1982 version of the code DWUCK4 which was used in the present work.

The experimental angular distributions from which the C^2S values were extracted are shown with the corresponding DWBA calculations in Figs. 2 and 3, for the bound and proton-unbound states, respectively. The C^2S values from this local, zero-range, $r_0=1.25$ fm analysis are presented in Table I. The uncertainties of the DWBA analysis are estimated to contribute a 20% systematic uncertainty to the C^2S values of the most strongly populated levels; this uncertainty can be considerably larger in the case of the weakly populated levels which have poor statistics and for which the single-step reaction model might be a poor approximation.

Although the values of the j transfers are determined unambiguously for the weakly populated levels at 3295, 3506, 4783, and 5115 keV from the knowledge of the J^π values, the l values are presented in parentheses in Table I because the fits of DWBA curves to the data are poor (Fig. 2). The spectroscopic factor of a proton-unbound state can be related to the proton partial width of the state through the relationship $C^2S=\Gamma_p/\Gamma_{\text{s.p.}}$, where $\Gamma_{\text{s.p.}}$ is the single-particle width which is calculated by the code DWUCK4. The spectroscopic factors from this work are compared in Table II with the spectroscopic factors which are deduced from the Γ_p values measured in the high-resolution study of the ^{30}Si(p,p)^{30}Si reaction,[7] quoted in the Introduction. It can be seen that the agreement is rather good for the C^2S values which are greater than about 0.04. Below this value the ratio of the C^2S values from the two determinations can be substantially different from unity. However, it must be kept in mind that for these levels the spectroscopic factors are obtained with accuracies which can be much worse than 20%.

Also in Table I the C^2S values from this work are compared with the values deduced from other stripping reactions.[1-5] For the ground state, the presently determined value is higher than any of the previous results. A large spread of the deduced C^2S values is observed for the 1266 keV level; for the other strongly excited levels there is overall agreement between the C^2S values from the various measurements. However, some significant discrepancies may be noticed. The J^π value of the $l=1$ level at 6496 keV is assumed to be $\frac{1}{2}^-$ in Ref. 2 and $\frac{3}{2}^-$ in this and the other works: the discrepancy is thus reduced, since the comparison of the experimental and calculated cross sections leads to the relationship $C^2S(j=l-\frac{1}{2})\approx 2C^2S(j=l+\frac{1}{2})$. The levels at 4190 and 4260 keV were not resolved in the work at 18 MeV (Ref. 3) because of an instrumental resolution of 70 keV, so the peak which is attributed there to the 4260 keV level corresponds in fact essentially to the more strongly populated level at 4190 keV. The C^2S value for the level at 7141 keV, $J^\pi=\frac{1}{2}^+$, $T=\frac{3}{2}$, is much higher in Ref. 3 than in the other works. This could be due to the fact that in that work the experimental angular distribution was measured only for $\theta_{\text{lab}}>30°$; this point exhibits the importance of the forward angles to get a reliable spectroscopic factor in the case of an $l=0$ transition.

For the $T=\frac{3}{2}$ states, the C^2S values from the (d,n) reaction are smaller than the values from the (^{3}He,d) reaction. This discrepancy already has been pointed out by the authors of Ref. 18.

It has been noted in the preceding section that the experimental angular distribution could be measured for the main component of a peak which actually incorporates the population of a multiplet of levels. In some cases the main component may itself correspond to a doublet of levels. Another analytical procedure was attempted for cases such as these, by considering a superposition of several DWBA angular distributions weighted by the spectroscopic factors. No more than two different transfers were considered in this procedure and only those examples in which a significant improvement was obtained in the reproduction of the experimental shapes were retained (levels at 8243–8247 keV and 8552-8556 keV). However, it must be kept in mind that the experimental angular distributions are not perfectly reproduced by the DWBA calculations even in the cases where only one l transfer is involved. Therefore, the accuracy is thought to be worse for the spectroscopic factors obtained through this alternative procedure, and they are presented in parentheses in Table I. The individual contributions of each transfer are also presented in Fig. 3.

This procedure was also used for the peaks which appear in Fig. 1 with excitation energies greater than 9.7 MeV and which were analyzed with the code HYPOGRAF. The experimental angular distributions are presented in Fig. 4 along with the DWBA predictions. These four peaks were identified with levels or groups of levels observed in the ^{30}Si(p,p)^{30}Si reaction[7] by comparing the transferred orbital angular momenta and the spectroscopic factors deduced from each reaction (Table II). The experimental angular distributions of the peaks at 9800 and 9950 keV are quite well accounted for by unique orbital angular momentum transfers. The broad peak at 9800 keV is identified with the broad level at 9787 keV seen in the (p,p) reaction because it is populated through an $l=1$ transfer [Fig. 4(d)], even though the C^2S value from the present work is substantially smaller than the value from Ref. 7. The peak at 9950 keV is identified with the level seen in (p,p) at 9946 keV since its angular distribution has a well-defined $l=3$ shape [Fig. 4(f)], even though the peak is observed only at the seven forward angles due to the proximity of the edge of the counter.

The experimental angular distributions of the peaks at 9720 and 9830 keV are well reproduced by mixtures of $l=1$ and $l=3$ transfers [Figs. 4(c) and 4(e), respectively]. Although the C^2S values from this work are only in moderate agreement with the values deduced from the Γ_p values of Ref. 7, the peak in the present work at 9720 keV is identified with the levels at 9719 and 9722 keV, and that at 9830 keV with the levels at 9815, 9818, 9820, and 9840 keV. However, from the Γ_p values[7] presented in

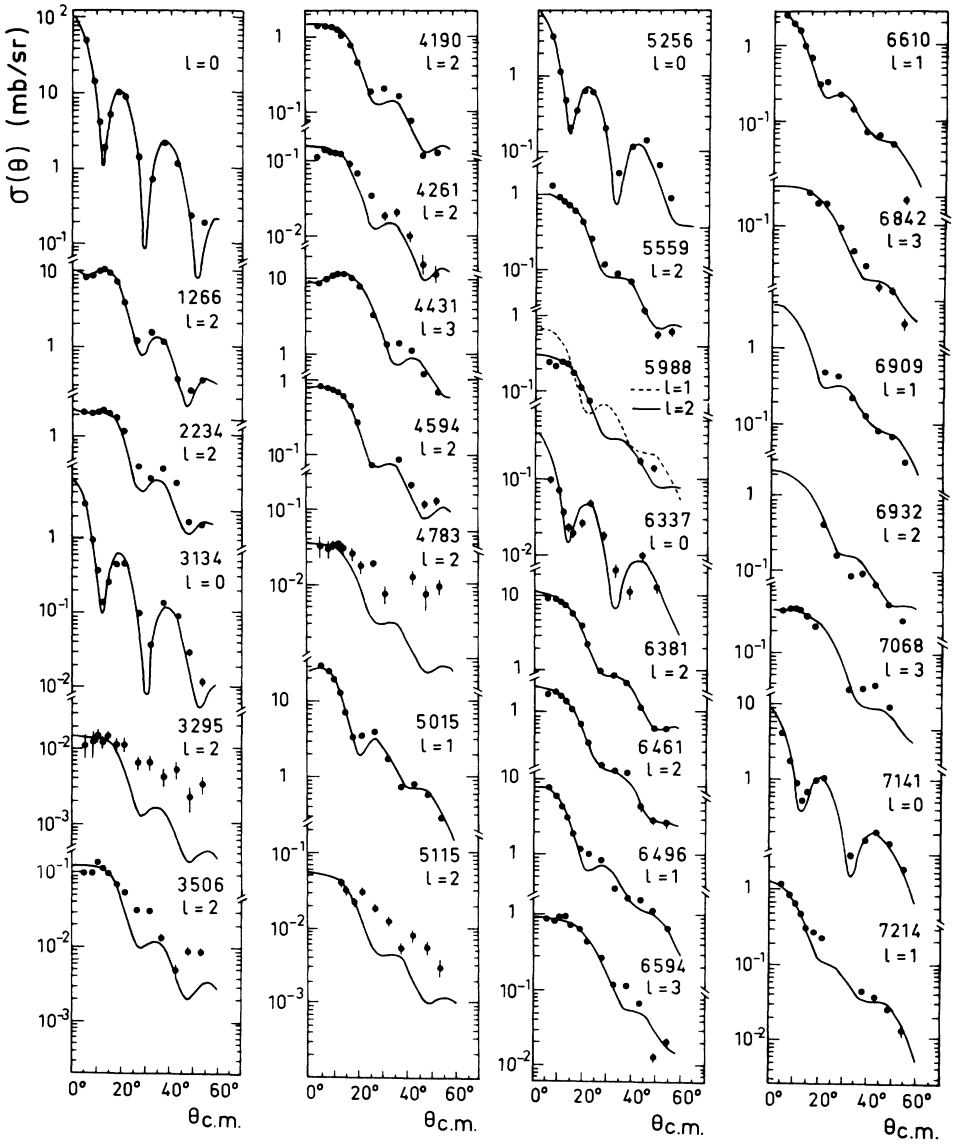

FIG. 2. Angular distributions from the ^{30}Si(^{3}He,d)^{31}P reaction leading to proton-bound states. If not shown, the error is less than the point size. Curves are DWBA predictions for the indicated l values. As for the two curves drawn for the level at 5988 keV, see text, Sec. V B.

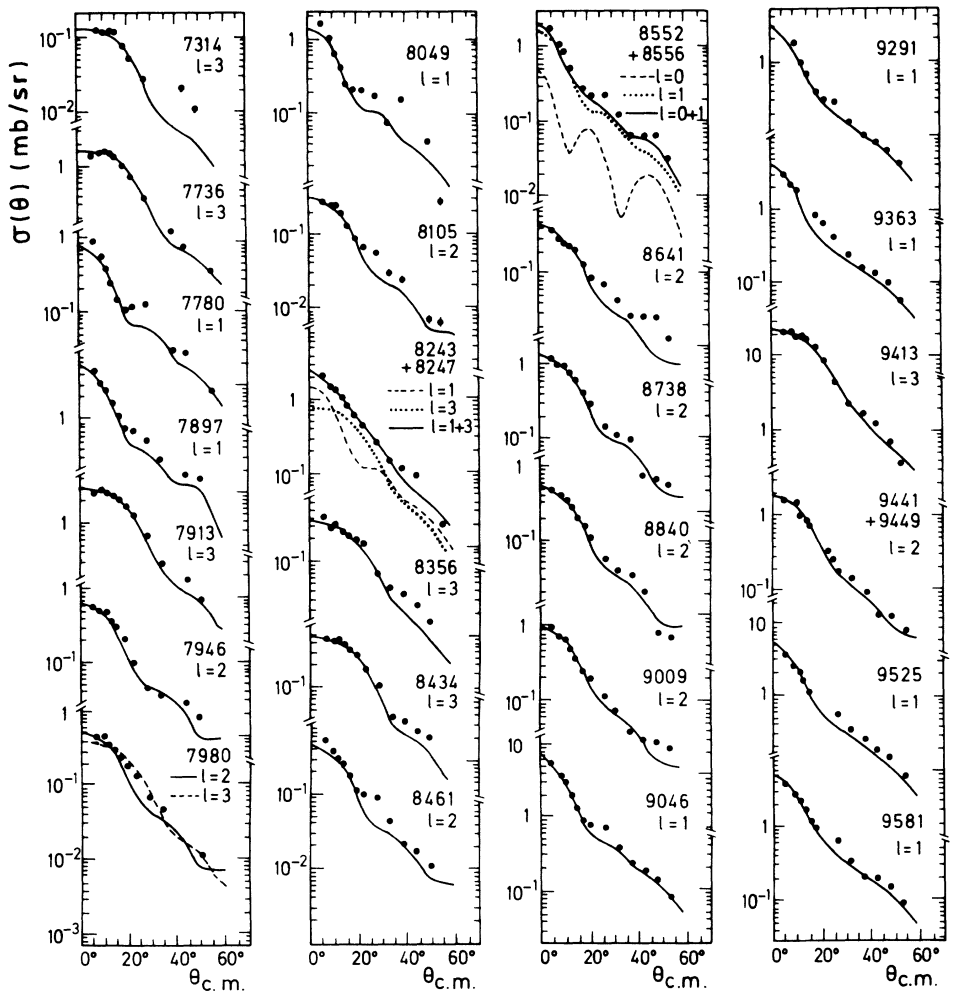

FIG. 3. Angular distributions from the ^{30}Si(^{3}He,d)^{31}P reaction leading to proton-unbound states. If not shown, the error is less than the point size. Curves are DWBA predictions for the indicated l values. For the groups of levels at 8.25 and 8.56 MeV, the contribution of different l transfers is also presented.

TABLE II. Comparison of the C^2S values from the present work and from the ^{30}Si(p,p)^{30}Si reaction (Ref. 7).

E_x (keV)[a]	l_p[b]	$J^\pi;T$[a]	Γ_p (eV)	$\Gamma_{s.p.}$ (keV)	C^2S (p,p)	C^2S (^{3}He,d)
8461	2	$\frac{5}{2}^+$	2±1	0.93	0.002	0.004
8544	1	$\frac{1}{2}^-$	54±10	19.2	0.003	
8552	0	$\frac{1}{2}^+$	313±35	51.8	0.006	(0.02)
8556	1	$\frac{3}{2}^-$	210±25	21.4	0.010	(0.01)
8576	2	$\frac{5}{2}^+$	7±5	1.74	0.004	
8584	1	$\frac{1}{2}^-$	50±10	22.9	0.002	
8641	2	$\frac{5}{2}^+$	5±3	2.38	0.002	0.004
8738	2	$\frac{3}{2}^+;\frac{3}{2}$	20±5	3.04	0.007	0.020
8757	2	$\frac{5}{2}^+$	3±2	3.97	0.001	
8763	0	$\frac{1}{2}^+$	1450±150	109	0.013	
8840	3	$\frac{7}{2}^-$	1±1	0.36	0.003	0.004
8903	0	$\frac{1}{2}^+$	90±15	162	0.001	
8910	2	$\frac{5}{2}^+$	1±1	7.16	<0.001	
8936	2	$\frac{3}{2}^+$	3±2	6.54	0.001	

TABLE II. (*Continued*).

E_x (keV)[a]	l_p[b]	$J^\pi;T$[a]	Γ_p (eV)	$\Gamma_{s.p.}$ (keV)	C^2S (p,p)	C^2S (^{3}He,d)
9009	2	$\frac{5}{2}^+;(\frac{3}{2})$	65±20	10.1	0.006	0.008
9046	1	$\frac{3}{2}^-$	9 300±940	110	0.085	0.070
9067	2	$\frac{5}{2}^+;(\frac{3}{2})$	16±5	12.1	0.001	
9114	3	$\frac{7}{2}^-$	1±1	1.07	0.001	
9116	2	$\frac{5}{2}^+;(\frac{3}{2})$	22±7	14.1	0.002	
9129	2	$\frac{5}{2}^+;(\frac{3}{2})$	3±2	14.7	<0.001	
9131	2	$\frac{5}{2}^+;(\frac{3}{2})$	4±2	14.7	<0.001	
9176	1	$\frac{3}{2}^-$	80±15	150	<0.001	
9227	1	$\frac{1}{2}^-$	4 000±400	162	0.025	
9241	2	$\frac{3}{2}^+$	150±15	16.9	0.009	
9253	3	$\frac{7}{2}^-$	3±1	1.72	0.002	
9291	1	$\frac{3}{2}^-$	9 800±1000	193	0.051	0.038
9363	1	$\frac{3}{2}^-$	10 000±1000	223	0.045	0.050
9400	0	$\frac{1}{2}^+$	500±75	471	0.001	
9413	3	$\frac{7}{2}^-;(\frac{3}{2})$	500±75	2.79	0.179	0.210
9441	2	$\frac{3}{2}^+$	180±20	28.1	0.006	0.015
9449	2	$\frac{5}{2}^+$	450±25	33.9	0.013	
9525	1	$\frac{3}{2}^-$	22 000±2000	302	0.073	0.065
9537	2	$(\frac{3}{2},\frac{5}{2})^+$	15±10	35.1[c]	<0.001	
9578	2	$(\frac{3}{2},\frac{5}{2})^+$	22±10	38.4[c]	0.001	
9581	1	$\frac{3}{2}^-$	20 000±2000	333	0.060	0.072
9585	0	$\frac{1}{2}^+$	3 800±400	640	0.006	
9719	3	$(\frac{5}{2},\frac{7}{2})^-$	30±10	6.24[d]	0.005	0.017[e]
9722	1	$\frac{3}{2}^-$	24 000±2000	418	0.057	0.027[e]
9756	2	$(\frac{3}{2},\frac{5}{2})^+$	3±2	55.2[c]	<0.001	
9760	2	$(\frac{3}{2},\frac{5}{2})^+$	20±7	55.4[c]	<0.001	
9766	1	$(\frac{3}{2})^-$	300±70	446	0.001	
9766	2	$(\frac{3}{2})^+$	200±50	55.6	0.004	
9787	1	$\frac{3}{2}^-$	50 000±5000	460	0.109	0.067
9815	3	$(\frac{5}{2},\frac{7}{2})^-$	12±5	7.80[d]	0.002	
9818	1	$\frac{3}{2}^-$	150±20	482	<0.001	
9820	1	$\frac{3}{2}^-$	4 500±450	483	0.009	0.028[e]
9840	3	$(\frac{7}{2})^-$	66±15	8.26	0.008	0.007[e]
9844	2	$(\frac{3}{2},\frac{5}{2})^+$	50±10	65.2[c]	0.001	
9869	1	$\frac{3}{2}^-$	350±35	518	0.001	
9908	1	$\frac{3}{2}^-$	350±35	547	0.001	
9929	2	$\frac{5}{2}^+$	170±20	88.8	0.002	
9946	3	$(\frac{5}{2})^-$	125±15	7.44	0.017	0.014

[a]Reference 12 for $E_x < 9.7$ MeV; Ref. 7 for higher excitation energies.
[b]Reference 7.
[c]Calculated with the assumption of $J^\pi = \frac{3}{2}^+$.
[d]Calculated with the assumption of $J^\pi = \frac{7}{2}^-$.
[e]These C^2S values were obtained by using the superposition procedure (see Sec. IV).

TABLE III. Optical model parameters used in DWBA calculations.

Channel	V (MeV)	r_r (fm)	a_r (fm)	W_V (MeV)	$4W_D$ (MeV)	r_i (fm)	a_i (fm)	$V_{s.o.}$ (MeV)	$r_{s.o.}$ (fm)	$a_{s.o.}$ (fm)	r_c (fm)
^{30}Si+^{3}He	189.8	1.15	0.669	24.0		1.495	0.886				1.40
^{31}P+d	85.7	1.17	0.755	0.9	48.0	1.325	0.749	6.55	1.07	0.66	1.30
Proton bound state	a	1.25	0.65					6.25	1.25	0.65	1.25

[a]The depth is adjusted by the code DWUCK4 for bound as well as unbound states.

Table II it can be inferred that the peak at 9830 keV arises mainly from the population of the 9820 and 9840 keV levels. From the identification of the peak at 9800 keV (this work) with the 50 keV wide level at 9787 keV (Ref. 7) it can be deduced that this level also contributes to the population of the peak at 9830 keV. It can thus be expected that the C^2S values from the present work for the $l=1$ transitions are smaller for the peak at 9800 keV (and larger for the peak at 9830 keV) than in Ref. 7.

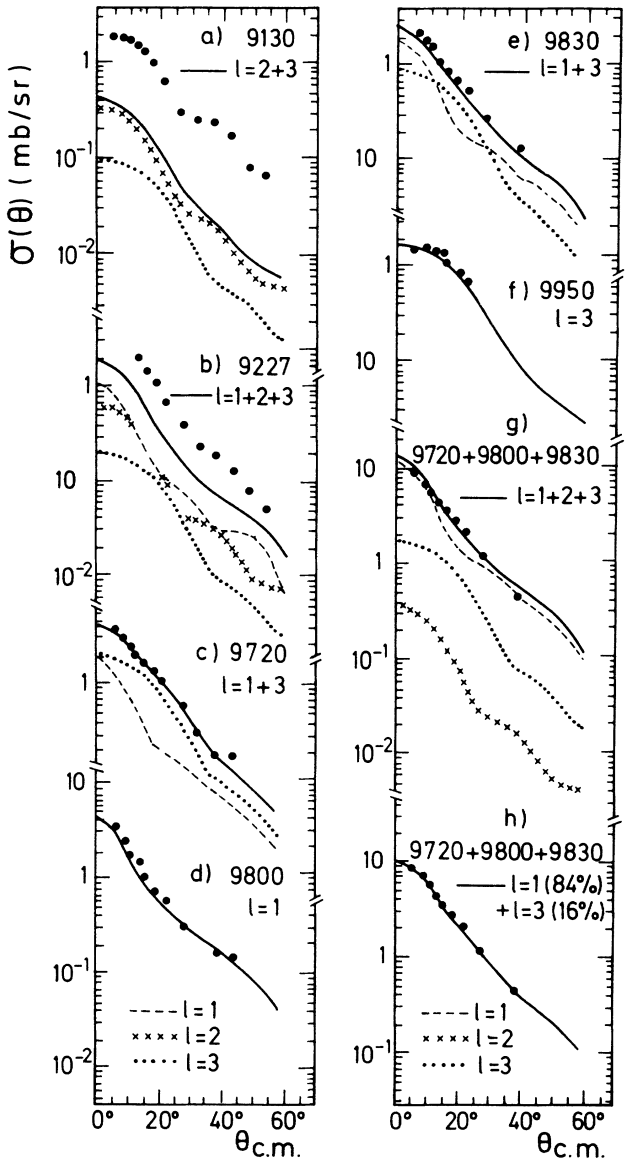

FIG. 4. Angular distributions from the ^{30}Si(^{3}He,d)^{31}P reaction leading to the peaks at 9130, 9247, 9720, 9800, 9830, and 9950 keV [parts (a)–(f)]. The summed angular distribution of the three peaks at 9720, 9800, and 9830 keV is also presented [parts (g) and (h)]. Curves are DWBA predictions resulting either from a unique l transfer or from the superposition of several l transfers. In this case the contribution of the various transfers is also presented. In the case of the level at 9247 keV the dashed-dotted curve results from the superposition of a revised $l=3$ contribution to the fixed $l=1$ and $l=2$ contributions (see text, Sec. IV).

Another analysis was carried out by considering the three peaks at 9720, 9800, and 9830 keV as a single group. The difficulty noted above, of extracting spectroscopic factors for each member of a group with the same accuracy as can be achieved in the case of an unique l transfer, can be illustrated through this analysis. In the 9.70–9.84 MeV excitation energy range, 12 levels were observed in the ^{30}Si(p,p)^{30}Si reaction:[7] five $l=1$ levels (three of them being several keV's wide), four $l=2$ and three $l=3$ levels. It can be seen in Fig. 4(g) that the experimental angular distribution obtained by means of the code HYPOGRAF for the sum of the three presently observed peaks is correctly reproduced by the superposition of the 12 relevant DWBA predictions weighted by the C^2S values deduced from the Γ_p measurements.[7] The summed contributions of the various l transfers are also presented in the same figure. This experimental angular distribution was also analyzed by combining the DWBA predictions corresponding to the two major l transfers ($l=1$ and $l=3$). The experimental points are correctly reproduced assuming a contribution of 84% for the $l=1$ transfer [Fig. 4(h)]. The C^2S values are 0.12 and 0.024 for $l=1$ and $l=3$, respectively, and they are to be compared with 0.17 and 0.015 obtained by summing the values from the (p,p) reaction (Table II). The comparison of the C^2S values for the $l=1$ transitions can be taken as an indication of the accuracy with which the spectroscopic factors are obtained in the superposition procedure, since it has been previously noted that the C^2S values from the (^{3}He,d) and (p,p) reactions are in good agreement as long as they are greater than 0.04.

Spectroscopic factors could not be obtained for the levels at 7718, 8208, 8225, 8576, 8601, and 8757 keV. These correspond to the weakest components of peaks due to the population of multiplets of levels. Likewise, spectroscopic factors could not be extracted for the seven peaks whose experimental angular distributions are displayed in Fig. 5. The peaks observed at 9130 and 9247 keV also could not be analyzed by using the code PICOTO. More than two levels are thought to be involved in the population of the peak at 9130 keV because the experimental angular distribution cannot be reproduced either by a unique l transfer or by any combination of two l transfers. Three $J^\pi=\frac{5}{2}^+$ and one $J^\pi=\frac{7}{2}^-$ levels have been observed[7] around 9130 keV, at 9114, 9116, 9129, and 9131 keV, respectively. The C^2S values which are deduced from the Γ_p values of Table II lead to cross-section predictions which are in disagreement with the experimental ones [Fig. 4(a)] in shape and in magnitude (by a factor of 5).

The three levels observed in Ref. 7 at 9227, 9241, and 9253 keV, with $J^\pi=\frac{1}{2}^-$, $\frac{3}{2}^+$, and $\frac{7}{2}^-$, respectively, can contribute to the population of the peak at 9247 keV. This peak is obscured at the three most forward angles by the intense peak resulting from the population of the two levels at 3509 and 3547 keV in the ^{12}C(^{3}He,d)^{13}N contaminant reaction. However, the magnitude of the cross sections which are predicted by using the C^2S values deduced from the Γ_p values of Table II is too low by a factor of 2.5 when compared with the experimental results

at larger angles [Fig. 4(b)]. It can be noted that the relative weight of the experimentally measured $l=1$ and $l=3$ transitions is not the same in this excitation energy range for the (^{3}He,d) and the (p,p) reactions. In the transfer reaction, the values at the first maximum of the calculated cross sections are about 26 mb/sr and 9 mb/sr for the $1f_{7/2}$ and $2p_{1/2}$ transfers, respectively, and the resulting peaks will be of comparable size if the C^2S values are similar. However, due to important differences in the Coulomb penetrabilities of the proton waves, the proton width will be much smaller for an $l=3$ level than for an $l=1$ level, even though these levels have similar C^2S values. As a result, the interference patterns in the elastic scattering experiments will be much more marked (and therefore the extracted Γ_p value more accurate) for the $l=1$ levels than for the $l=3$ levels. Therefore it was attempted to account for the experimental angular distribution of the 9247 keV peak by keeping fixed the C^2S values of Table II for the $J^\pi=\frac{1}{2}^-$ and $\frac{3}{2}^+$ levels and by varying only the contribution of the $J^\pi=\frac{7}{2}^-$ level. In contrast with the case of the level at 9130 keV, good agreement in shape and in magnitude can thus be obtained by using a value $C^2S=0.015$ for the $l=3$ transfer [Fig. 4(b), dashed-dotted curve]. Such a value would lead to a proton width ($\Gamma_p=23$ eV) eight times larger than the value of Ref. 7.

The occurrence of another reaction process with a low cross section is evidenced through the population of the levels at 6796 and 6825 keV, which have been assigned $J^\pi=\frac{9}{2}^-$ and $\frac{11}{2}^-$, respectively, in Ref. 12. A direct one-step process would involve the high-lying $1h_{9/2}$ and $1h_{11/2}$ shells. The shapes of the experimental angular distributions are not reproduced (Fig. 6) by DWBA calculations done with the assumption of a one-step $l=5$ transfer, a process which furthermore would be quite unlikely at these energies. A similar situation is found with the experimental angular distributions of two $J^\pi=\frac{7}{2}^+$ and three $J^\pi=\frac{9}{2}^+$ levels. These also are not well reproduced with the assumption of a one-step $l=4$ transfer (Fig. 6).

The C^2S values corresponding to the various l transfers are displayed in Fig. 7 vs the excitation energy. For this figure the C^2S values deduced from Ref. 7 were adopted for the three levels at 9722, 9787, and 9820 keV. It is thought that the measurements of the Γ_p values for these three broad $l=1$ levels are more accurate with the (p,p) experiment than with the present experiment in which they are obtained either directly for the level at 9787 keV (the importance of which can be underestimated as indicated above) or through the superposition procedure for the levels at 9722 and 9820 keV. It can be seen in Fig. 7 that essentially one $T=\frac{1}{2}$ and one $T=\frac{3}{2}$ level is strongly populated through each of the l transfers 0, 2, and 3. In contrast, many levels are observed with $l=1$ transfer. A similar situation was previously observed for the ^{30}P and ^{32}S nuclei (Refs. 19 and 13, respectively). The concentration of strongly excited $l=1$ levels between 9.0 and 9.8 MeV in ^{31}P was also previously reported in Ref. 7.

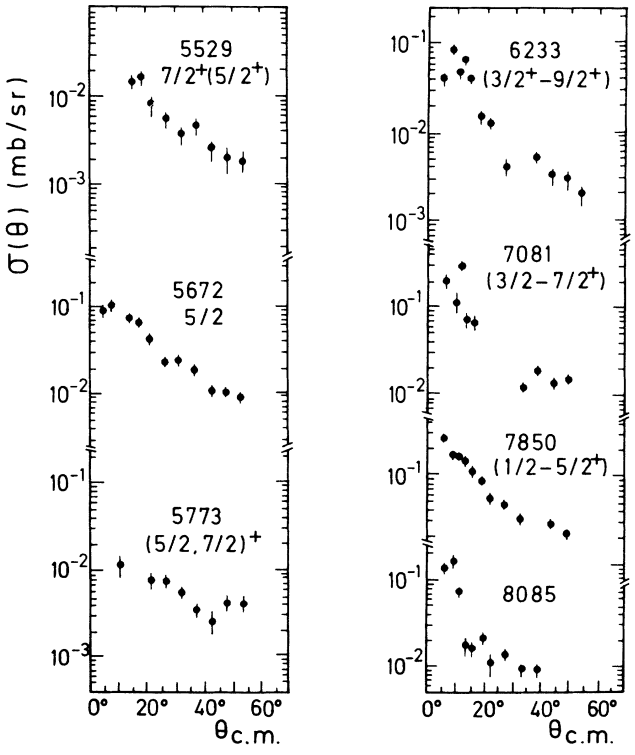

FIG. 5. Angular distributions from the ^{30}Si(^{3}He,d)^{31}P reaction which are not reproduced by the DWBA calculations.

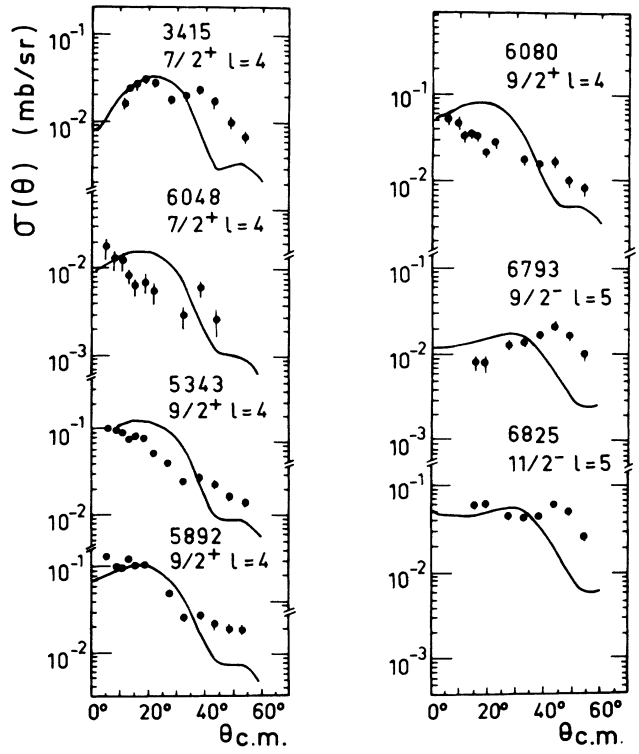

FIG. 6. Angular distributions from the ^{30}Si(^{3}He,d)^{31}P reaction which are not well reproduced by the DWBA calculations. Curves are DWBA predictions for the indicated l values, which are consistent with the J^π values of the levels.

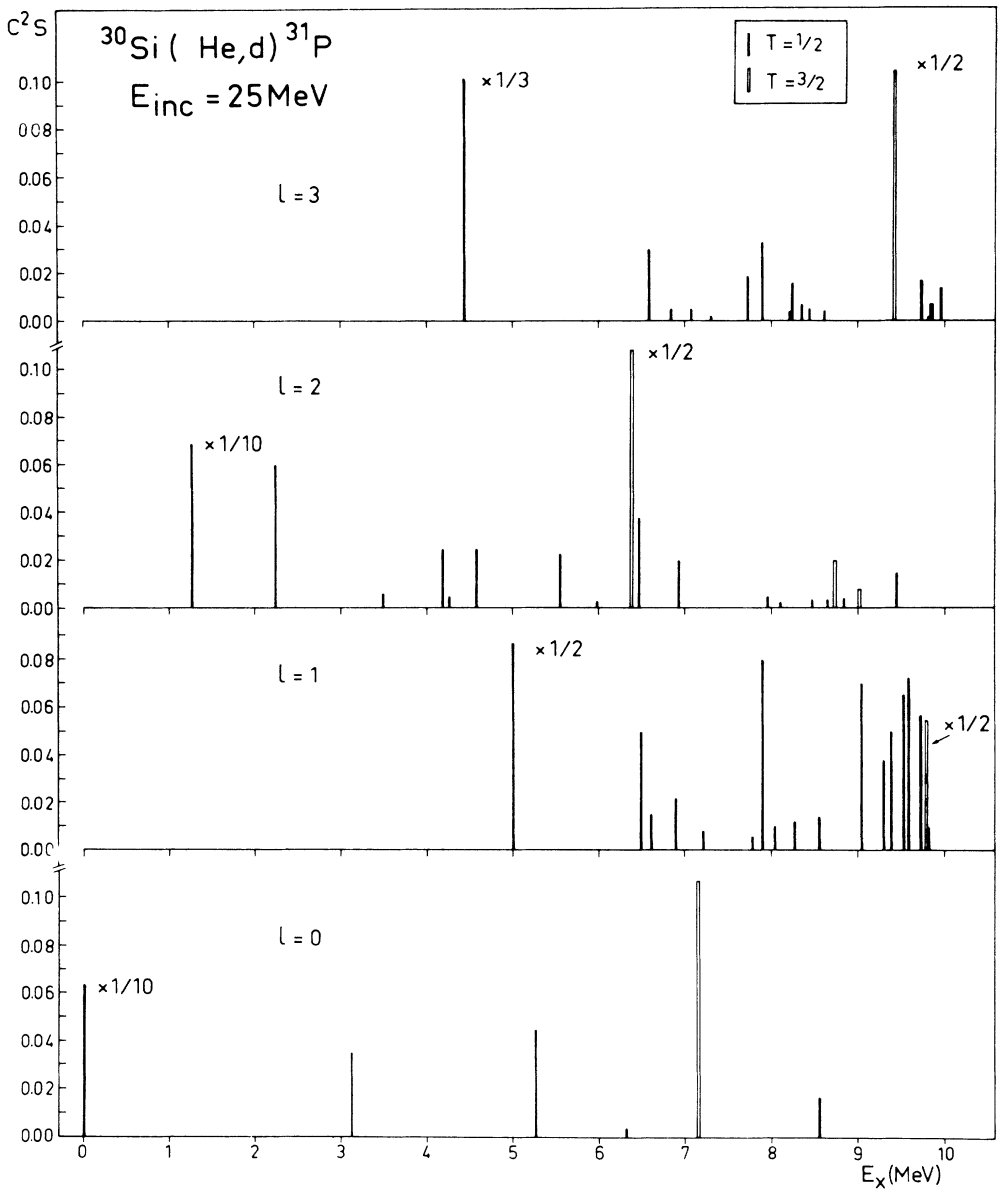

FIG. 7. Strength distribution for the $l=0$, 1, 2, and 3 transfers. Solid bars indicate $T=\frac{1}{2}$ transitions and open bars $T=\frac{3}{2}$ transitions. The C^2S values for the $l=1$ transitions to the levels at 9722, 9787, and 9821 keV are calculated from the Γ_p values of Ref. 7 presented in Table II.

V. DISCUSSION OF MISCELLANEOUS RESULTS

A. New energy levels

The width of the peak which appears at an excitation energy of about 7.9 MeV in Fig. 1 is larger than the 23 keV instrumental resolution. The same method of analysis as described in Sec. III for the peak at 6.6 MeV was used for the peak at 7.9 MeV. This analysis shows that this peak is due to the population of two levels, at 7897 and 7913 keV, excited through $l=1$ and $l=3$ transfers, respectively (Fig. 3). The $l=1$ assignment to the level at 7897 keV level is in agreement with Ref. 5. The level at 7913 keV is observed here for the first time in a single-proton stripping reaction. From its $l=3$ angular distribution, values of $J^\pi=(\frac{5}{2},\frac{7}{2})^-$ spin and parity are proposed for this level. It may be the same as the level observed at 7911±5 keV in a high-resolution study of the ^{29}Si$(\alpha,d)^{31}$P reaction at 37.5 MeV.[20] It is likely also that this level was observed in a study at 15 MeV of the ^{29}Si$(^3$He$,p)^{31}$P reaction.[21] The experimental angular distribution of a peak at 7895 keV could be reproduced with the assumption of $L=2$ or $L=1+3$ for the transferred neutron-proton pair. So this peak can be due to the population of the two levels at 7897 and 7913 keV. Besides the level at 7913 keV, three others, at excitation energies of 7068, 7736, and 7980 keV, were also observed for the first time in the present work.

B. Angular momenta and parities

The value of the transferred orbital momentum l which is obtained from an analysis of a (^{3}He,d) angular distribution measurement leads to one value for the parity [$\pi=(-1)^l$] and two possible values for the total angular momentum ($J=l\pm\frac{1}{2}$) of the populated level. The previously known J^π values from Refs. 7 and 12 are adopted in Table I when they are in agreement with the conclusions of the present work. The present determination of l-transfer values has made possible parity assignments to the levels at 8107, 8355, and 8433 keV, since only their spin J values were previously known.

The J^π assignments of the present work are in disagreement with previous determinations for the levels at 5988, 7314, and 8840 keV. The 5988 keV level was assigned $J^\pi=\frac{3}{2}^-$ in Ref. 1. This assignment was not deduced from the DWBA analysis of an angular distribution because the relevant peak was observed at only three forward angles, but it relied upon the identification of the level with a level excited through an $l=1$ proton pickup in the ^{32}S(d,^{3}He)^{31}P reaction[22] and upon the γ-decay properties of this state. However, it was suggested in a more recent and higher resolution study of the same pick-up reaction[23] that the population of the 5988 keV level was due more likely to an $l=2$ proton pickup. In the present work the peak corresponding to the 5988 keV level could be separated at almost all the angles from the peak due to the level at 1384 keV formed in the ^{28}Si(^{3}He,d)^{29}P contaminant reaction. The DWBA analysis leads to an $l=2$, $J^\pi=(\frac{3}{2},\frac{5}{2})^+$ assignment, in agreement with Ref. 23. The DWBA shape of an $l=1$ transfer is also presented for comparison in Fig. 2.

On the other hand, the discrepancies for the 7314 and 8840 keV levels are not understood. For these levels the proton l transfers from the present work lead to $J^\pi=(\frac{5}{2},\frac{7}{2})^-$ and $(\frac{3}{2},\frac{5}{2})^+$ assignments, respectively, whereas the $J^\pi=(\frac{1}{2}\text{-}\frac{5}{2}^+)$ and $\frac{7}{2}^-$ assignments, respectively, were proposed in Ref. 12, based on electromagnetic decay properties. An $L=0$ transition to the 7314 keV level was observed[21] in the ^{29}Si(^{3}He,p)^{31}P reaction, which leads to a $J^\pi=(\frac{1}{2},\frac{3}{2})^+$ assignment for this level, in agreement with Ref. 12.

C. Isospin assignments

Levels in ^{31}P have been proposed[7,12] as the analog states of the first seven states of ^{31}Si. Because of isospin symmetry, the proton and neutron spectroscopic factors, respectively, should be the same for corresponding states in ^{31}P and ^{31}Si. This comparison is presented in Table IV along with the excitation energy differences $\Delta E_x=E_x(^{31}\text{P})-E_x(^{31}\text{Si})$ which corresponds to the Coulomb energy differences minus the neutron-proton mass difference.

The agreement between spectroscopic factors is good for the levels at 6381, 7141, 8738, and 9413 keV in ^{31}P and the levels at 0, 752, 2317, and 3134 keV in ^{31}Si, respectively. The value of ΔE_x is about the same for the three even-parity levels, the mean value being 6397 keV. This quantity is substantially smaller (6279 keV) for the odd-parity state. A similar effect has been observed previously for the $l=1$ and $l=3$ states in the $A=32$ (Ref. 13) and $A=36$ (Ref. 25) nuclei. The analog state of the 3534 keV level in ^{31}Si, $J^\pi=\frac{3}{2}^-$, would thus be expected in ^{31}P at about 9800 keV. The broad level at 9787 keV has been tentatively proposed as this state. The spectroscopic factor S_p which is deduced from the Γ_p value[7] is in good agreement with the S_n value from Ref. 24.

It is difficult to identify in ^{31}P the analogs of the levels

TABLE IV. A comparison of the spectroscopic information in ^{31}Si and ^{31}P.

^{31}Si[a]				^{31}P[b]					
E_x (keV)	J^π	l_n	$(2J+1)S_n$	E_x (keV)	J^π	l_p	$(2J+1)S_p$		ΔE_x (keV) $=E_x(^{31}\text{P})$-$E_x(^{31}\text{Si})$
0	$\frac{3}{2}^+$	2	3.4	6381	$\frac{3}{2}^+$	2	2.59		6381
752	$\frac{1}{2}^+$	0	0.54	7141	$\frac{1}{2}^+$	0	0.64		6389
1695	$\frac{5}{2}^+$	2	0.12	8032	$\frac{5}{2}$		[c]		6337
				8105	$\frac{5}{2}^+$	2	0.05		6410
2317	$\frac{3}{2}^+$	2	0.24	8738	$\frac{3}{2}^+$	2	0.24		6421
2789 or	$\frac{5}{2}^+$	2	0.24	9009	$\frac{5}{2}^+$	2	0.112	0.17[d]	6251
				9067	$\frac{5}{2}^+$		0.023		
				9116	$\frac{5}{2}^+$		0.027		
				9129	$\frac{5}{2}^+$		0.004		
				9131	$\frac{5}{2}^+$		0.005		
2789	$\frac{3}{2}^+$	2	0.16	9241	$\frac{3}{2}^+$		0.11[d]		6452
3134	$\frac{7}{2}^-$	3	4.4	9413	$\frac{7}{2}^-$	3	5.0		6279
3534	$\frac{3}{2}^-$	1	1.9	9787	$\frac{3}{2}^-$	1	1.3[d]		6253

[a]References 12 and 24.
[b]This work and Refs. 7 and 12.
[c]Not observed in this work.
[d]Calculated from the Γ_p values of Ref. 7.

of ^{31}Si which carry only a small fraction of the single-particle strength. This is the case for the ^{31}Si levels at 1695 and 2789 keV, $J^\pi=\frac{5}{2}^+$ and $\frac{5}{2}^+(\frac{3}{2}^+)$, respectively. The two levels at 8032 and 8107 keV, $J=\frac{5}{2}$, were tentatively proposed[12] as analogs of the ^{31}Si level at 1695 keV. For these two levels the ΔE_x values are equal to 6337 keV and 6410 keV, respectively, in reasonable agreement with the 6397 keV mean value. The level at 8032 keV is not observed in this work because a strong peak, arising from the level at 3447 keV formed in the ^{28}Si(^{3}He,d)^{29}P contaminant reaction, appears in that energy region. Even parity is deduced from this work for the weakly excited level at 8107 keV. Keeping in mind the lack of accuracy for such a small spectroscopic factor, this result is not strongly at variance with the spectroscopic factor of the 1695 keV level in ^{31}Si. However, if even parity could be assigned to the 8032 keV, the assumption of the splitting of the analog strength between the two levels at 8032 and 8107 keV would be reinforced. With the assumption of the same spectroscopic factor for the two levels, a ΔE_x value of 6375 keV would be obtained, in excellent agreement with the mean value.

It has been suggested[7,12] that the analog state of the 2789 keV level in ^{31}Si is split in ^{31}P over the five $J^\pi=\frac{5}{2}^+$ levels found at 9009, 9067, 9116, 9129, and 9131 keV. In the present work, a spectroscopic factor was measured only for the level at 9009 keV; therefore, the spectroscopic factors were obtained for these five levels from the Γ_p values of Ref. 7 presented in Table II. The summed value, $S_p=0.03$, compares reasonably well with the value $S_n=0.04$ (Ref. 24). In contrast, the centroid of the excitation energies weighted by the spectroscopic factors of these five levels is equal to 9040 keV, leading to a ΔE_x value of 6251 keV which is smaller than the mean value by more than 140 keV. It must be pointed out that the $J^\pi=\frac{5}{2}^+$ assignment to the ^{31}Si level rests only upon the J dependence of the $l=2$ angular distributions in the (d,p) reaction.[26] If the $J^\pi=\frac{3}{2}^+$ assignment is considered, the analog state could be the 9241 keV level. Since this spectroscopic factor was not obtained in the present work, the value $S_p=0.03$ was deduced from the Γ_p value of Ref. 7 (Table II). The ΔE_x value of 6452 keV would be in better agreement with the mean value.

D. Proton and total widths of the $J^\pi=\frac{1}{2}^-$ level at 7897 keV

This level is observed at $E_p=620$ keV in the ^{30}Si$(p,\gamma)^{31}$P reaction.[12] The $J=\frac{1}{2}$ assignment relies upon the isotropic angular distribution of the main transition to the ground state,[27] and the assignment of odd parity is from the population of the level through an $l=1$ transfer (this work and Ref. 5). The total width, $\Gamma=68\pm9$ eV, has been obtained in the ^{30}Si$(p,\gamma)^{31}$P reaction[28] through a resonant absorption measurement. A value of the resonance strength, $(2J+1)\Gamma_p\Gamma_\gamma/\Gamma=3.9\pm0.2$ eV, was measured in another study[29] of the same proton radiative capture reaction. Proton emission to the ^{30}Si ground state and gamma decay are the only decay channels open for this level. Therefore, $\Gamma=\Gamma_p+\Gamma_\gamma$ and the following values can be calculated by combining the values of the resonance strength and of the total width: Γ_p (or Γ_γ)$=66\pm9$ eV and Γ_γ (or Γ_p)$=2.0\pm0.2$ eV.

The value $\Gamma_p=66$ eV seems the more likely choice, because the alternative solution would lead to an $E1$ transition strength of 0.19 ± 0.03 Weisskopf units, which would exceed the most intense of the 566 other $E1$ transitions of the $A=21-44$ mass region[30] by more than a factor of 2. However, both solutions for Γ_p are in disagreement with the value $\Gamma_p=9\pm2$ eV which is deduced in this work from the value $C^2S=0.08$ by using the single-particle width $\Gamma_{s.p.}=104$ eV calculated for a $2p_{1/2}$ transfer. An accuracy of 20% is assumed for the spectroscopic factor. This C^2S value is in agreement with a previous result.[5] The discrepancy is not substantially reduced if the older value of Ref. 31 ($\Gamma=40\pm7$ eV) is used for the total width. A contribution to the solution of this puzzling point could be obtained by making an independent measurement of the Γ_p value through a careful study of the ^{30}Si$(p,p)^{30}$Si reaction around $E_p=620$ keV. A quite measurable effect should be observed for a level with a proton width as large as 66 eV.

VI. COMPARISON BETWEEN EXPERIMENTAL AND CALCULATED EXCITATION ENERGIES AND SPECTROSCOPIC FACTORS FOR POSITIVE-PARITY STATES

Recent shell-model calculations have succeeded in producing a unified and generally accurate reproduction of *sd*-shell nuclear structure. The general level of success of these calculations is motivation for attempting to critique their fundamental predictions with greater accuracy than has previously been feasible. The occupation probabilities of the model orbits in the middle of the shell, where all three are simultaneously near the Fermi surface, is one of the most fundamental and critical aspects of the model predictions. The spectroscopic factors for ^{30}Si(^{3}He,d)^{31}P are a key measure of these orbit occupancies.

Table V presents comparisons of the excitation energies and spectroscopic factors of 20 positive-parity levels studied in the present work with the shell-model predictions. In the energy comparisons, the lowest model states of $T=\frac{1}{2}$ and $T=\frac{3}{2}$ are set equal to the measured energies (0 keV and 6381 keV, respectively) in ^{31}P. The mean deviation between the measured and calculated excitation energies is equal to 147 keV, and the largest deviation is 364 keV.

The experimental observations show that most (91%) of the $2s_{1/2}$ and $1d_{3/2}$ strengths is concentrated into the lowest-lying $J^\pi=\frac{1}{2}^+$, $T=\frac{1}{2}$; $J^\pi=\frac{1}{2}^+$, $T=\frac{3}{2}$; $J^\pi=\frac{3}{2}^+$, $T=\frac{1}{2}$; and $J^\pi=\frac{3}{2}^+$, $T=\frac{3}{2}$ levels. This is in excellent agreement with the shell-model predictions, which also put 91% of the strength calculated for this region of excitation into these same four levels. However, Table V also indicates that the sum of the predicted strength for these four levels is only 80% of the sum of the experimental values. This is similar to the situation previously observed in the ^{32}S nucleus,[13] for which the ratio between the calculated and experimental summed spectroscopic factors was 0.75.

TABLE V. Comparison of experimental and calculated excitation energies and spectroscopic factors.

Shell-model calculations		Present work		$E_{x\,calc}-E_{x\,exp}$
E_x (keV)	100S	E_x (keV)	100S	(keV)
	$nlj=2s_{1/2}$ transitions to $T=\frac{1}{2}$ states			
0	76.9	0	95.6	0
3 310	5.3	3134	5.1	176
5 084	0.2	5015[a]		69
5 536	3.5	5256	6.8	280
6 531	0.8	6337	0.6	195
7 346	0.4			
7 921	0.0			
8 189	2.0	8552	2.6	−364
	$nlj=2s_{1/2}$ transitions to $T=\frac{3}{2}$ states			
7 196[b]	21.9	7141	32.1	55
10 874	7.5			
12 295	1.0			
13 025	0.0			
13 552	0.2			
13 756	0.0			
14 074	0.2			
14 485	0.0			
	$nlj=1d_{3/2}$ transitions to $T=\frac{1}{2}$ states			
1 210	81.3	1266	102.9	−56
3 587	0.1	3506	0.9	81
4 581	0.1	4261	0.8	320
4 733	6.4	4594	3.8	139
5 763	1.4	5559	3.5	204
6 117	0.8			
6 586	0.6			
7 159	0.9			
	$nlj=1d_{3/2}$ transitions to $T=\frac{3}{2}$ states			
6 381[b]	58.4	6381	64.8	0
8 676	2.7	8738	6.0	−62
10 206	4.4			
11 509	0.7			
12 090	0.1			
12 596	0.2			
12 698	0.5			
13 055	0.3			
	$nlj=1d_{5/2}$ transitions to $T=\frac{1}{2}$ states			
2 275	10.4	2234	9.0	41
3 297	0.1	3295	0.03	2
4 344	4.7	4190	3.8	154
4 866	0.0	4783	0.05	83
5 321	0.0	5115	0.07	206
5 968	0.1			
6 546	0.1			
6 801	0.0			
	$nlj=1d_{5/2}$ transitions to $T=\frac{3}{2}$ states			
7 987[b]	1.9	8105	0.9	−118
9 251	4.8	9009	2.4	242
11 418	0.1			
11 779	0.1			
12 145	0.9			
12 455	0.2			
13 021	0.1			
13 265	0.4			

[a]See text, Sec. VII A.

[b]All the energies which appear in this column for the $T=\frac{3}{2}$ levels were obtained by adding 6381 keV to the values from the shell-model calculation.

The absolute scale of values of experimentally based (^{3}He,d) spectroscopic factors should not be taken uncritically, however. As noted, approximate corrections for the effects of finite range and nonlocality can reduce the extracted spectroscopic factors by 25% and, in addition, the spectroscopic factors are reduced by about 3% for each increase of 0.01 fm in the radius of the potential which generates the proton form factor. Hence, the difference in absolute values of $S(s_{1/2})$ and $S(d_{3/2})$ are not necessarily meaningful. Much more pertinent are the agreements in the relative distributions of strength into specific states and energy regions and in the relative magnitudes of the four dominant states. On these grounds the model predictions are validated by the present results. In particular, the predicted relative occupancies of the $2s_{1/2}$ and $1d_{3/2}$ orbits appear correct.

The model predictions are less successful in predicting the occupancy of the $1d_{5/2}$ orbit in comparison to the present experimental results. If the magnitudes of the experimentally based $1d_{3/2}$ and $2s_{1/2}$ values of S are scaled down to match in sum the model predictions, then the $1d_{5/2}$ values would also be scaled down by essentially equal factors. This would result in the experimentally based occupancy of the $1d_{5/2}$ orbit appearing to be higher (smaller S factor) than is predicted by the model. Such a discrepancy cannot be explained away in terms of nondirect contributions to the observed cross sections. The implications of the $1d_{5/2}$ results are that the standard reaction model used here incorrectly treats the relative $1d_{5/2}$ and $1d_{3/2}$ cross-section magnitudes, or that the model occupancy for $1d_{5/2}$ is in error, or that a combination of both effects is occurring.

VII. COMPARISON WITH THE SUM-RULE LIMITS FOR THE ODD-PARITY STATES

Since there are no calculations of the individual spectroscopic factors for these states, the sums of the experimental spectroscopic strengths G_{lj} [where $G_{lj}=(2J+1)C^2S_{lj}$] are compared to the model-independent sum rules[6] for a stripping reaction

$$\sum G_{lj}(T=\tfrac{1}{2}) = \{\text{proton holes}\}_{lj} - \{\text{neutron holes}\}_{lj}/(N-Z+1)\ ,$$

$$\sum G_{lj}(T=\tfrac{3}{2}) = \{\text{neutron holes}\}_{lj}/(N-Z+1)\ ,$$

where N and Z are the neutron and proton numbers of the target. The sum-rule limits are $2(2j+1)/3$ and $(2j+1)/3$ for the isospin $T=\frac{1}{2}$ and $T=\frac{3}{2}$, respectively, in the case of empty orbits.

A. $j=\frac{3}{2}$ transitions

For this comparison the first component of the doublet at 5015 keV is assumed to have $J^\pi=\frac{3}{2}^-$ on the following grounds. First, the second component which is assigned $J^\pi=(\frac{1}{2},\frac{3}{2}^+)$ in Ref. 12 can be tentatively identified with the third $J^\pi=\frac{1}{2}^+, T=\frac{1}{2}$ level which is predicted at 5084 keV in the shell-model calculations (see Table V). Second, if this assumption is erroneous and if the two components are populated with $l=1$, the J^π value would be $\frac{1}{2}^-$ for the second component. However, the population of the two components with $l=1$ seems unlikely, because the presence at the same energy in ^{31}P of the first $2p_{3/2}$ and $2p_{1/2}$ states would be in contrast to the situation observed for neighboring sd-shell nuclei such as ^{27}Al, ^{29}P, ^{33}Cl, and ^{35}Cl, in which the first $2p$ state is $2p_{3/2}$ and the first $2p_{1/2}$ state lies higher by at least several hundreds of keV's.

The identification of the $2p_{3/2}$ transitions is unambiguous in the excitation energy range which is common with the (p,p) reaction because clearly distinct interference patterns are obtained for the $2p_{3/2}$ and $2p_{1/2}$ transfers in the case of an even-even target.[7] The observed $l=1$ strength has also been assumed to arise from a $2p_{3/2}$ transfer for the other states of ^{31}P for which J^π values have not been established previously. The contribution of $2p_{3/2}$ transitions may thus be overestimated. All the levels populated in an $l=1$ transfer were assigned $T=\frac{1}{2}$, with the exception of the level at 9787 keV (Sec. V C). The summed spectroscopic strengths of the 16 levels which are presented in Table VI reach a value of 2.68, in excellent agreement with the sum-rule limit. If the summation is restricted to 14 levels by excluding the levels at 6496 and 7214 keV for which the $J^\pi=\frac{3}{2}^-$ assignment is not unambiguously determined, a value of 2.44 is obtained. This result does not change the above conclusion, namely that the $2p_{3/2}$ single-particle strength is exhausted in the observed excitation range. Of this $2p_{3/2}$ observed strength, 80% are concentrated in the level at 5015 keV and the seven strongly populated levels which appear between 9.0 and 9.8 MeV. Whatever number of levels are considered (16, 14, or only the 8 most strongly populated ones), quite similar values are obtained for the centroid energy of the $2p_{3/2}$, $T=\frac{1}{2}$, configuration, namely 7821, 7937, or 7962 keV, respectively. The spectroscopic strength of the $J^\pi=\frac{3}{2}^-$, $T=\frac{3}{2}$ level at 9787 keV is 0.42 and corresponds to only 30% of the sum-rule limit.

B. $j=\frac{7}{2}$ transitions

The assumption of $j=l+\frac{1}{2}$ transfer has been made for all observed $l=3$ transitions to levels for which the J^π value is not uniquely determined. About 60% of the sum-rule limit is observed both for $T=\frac{1}{2}$ and $T=\frac{3}{2}$ states. The $T=\frac{1}{2}$ observed strength is distributed over nine states (Table VIc), whereas the $T=\frac{3}{2}$ observed strength is concentrated into only one level located at 9413 keV. However, since 80% of the $T=\frac{1}{2}$ observed strength is concentrated into the level at 4431 keV, it may be concluded that a dominant, and almost equal, portion of the $1f_{7/2}$ strength is concentrated into a single level of each isospin.

C. $j=l-\frac{1}{2}$ transitions

The level at 7897 keV is the only representative of the $2p_{1/2}$, $T=\frac{1}{2}$, configuration which is observed in this

TABLE VI. Spectroscopic strengths for the odd-parity levels.

E_x (keV)	$C^2S\times100$	$G\times100$
$nlj=2p_{3/2}$ transitions to $T=\frac{1}{2}$ states		
5015	17.3	69.2
6496	5.0	20.0
6610	1.5	6.0
6909	2.2	8.8
7214	0.8	3.2
7780	0.5	2.0
8049	1.0	4.0
8247	1.2	4.8
8556	1.4	5.6
9046	7.0	28.0
9291	3.8	15.2
9363	5.0	20.0
9525	6.5	26.0
9581	7.2	28.8
9722	5.6[a]	22.4
9820	0.9[a]	3.6
Sum rule limit: $\frac{8}{3}$		$\sum G=2.68$
$nlj=2p_{1/2}$ transitions to $T=\frac{1}{2}$ states		
7897	8.0	16.0
8544	0.3[a]	0.6
8584	0.2[a]	0.4
9227	2.5[a]	5.0
Sum rule limit: $\frac{4}{3}$		$\sum G=0.22$
$nlj=1f_{7/2}$ transitions to $T=\frac{1}{2}$ states		
4431	30.4	243.2
6842	0.5	3.9
7314	0.2	1.6
7736	1.9	15.3
7913	3.3	26.0
8434	0.5	3.8
9719	1.7	13.6
9815	0.2	1.6
9840	0.7	5.6
Sum rule limit: $\frac{16}{3}$		$\sum G=3.15$
$nlj=1f_{5/2}$ transitions to $T=\frac{1}{2}$ states		
6594	3.0	18.0
8243	1.5	9.2
8356	0.6	3.8
9946	1.4	8.4
Sum rule limit: 4		$\sum G=0.39$

[a]From the Γ_p values of Ref. 7.

work. The spectroscopic strength, 0.16, is only 12% of the sum-rule limit. If the levels at 6496 and 7214 keV are assigned $J^\pi=\frac{1}{2}^-$, the percentage of the sum-rule limit would reach about 30%. The situation for the $1f_{5/2}$ strength is quite similar to that of the $2p_{1/2}$ strength: only 10% of the sum-rule limit is observed for the $T=\frac{1}{2}$ case (Table VId). Most of the $2p_{1/2}$ and $1f_{5/2}$ missing strength can be expected to lie at excitation energies higher than the range of the present experiment, but some might also be distributed among ^{31}P levels below 10 MeV which escaped observation because they are too weakly populated or unresolved from neighboring levels.

The first ^{31}Si level which could belong to the $2p_{1/2}$ configuration is the $J^\pi=(\frac{1}{2},\frac{3}{2})^-$ level at 5874 keV. The analog of such a state would lie at an excitation energy higher than 12 MeV, which is considerably above the excitation range investigated in this work. It is also the case for the levels which belong to the $1f_{5/2}$, $T=\frac{3}{2}$, configuration.

VIII. SUMMARY

The present study has provided a comprehensive catalog of states populated by adding a proton to ^{30}Si. The results, when considered in conjunction with the results of a ^{30}Si(p,p)^{30}Si study, show that the preponderance of $l=0$, $l=2$, $l=1$ ($J=\frac{3}{2}$; $T=\frac{1}{2}$) and $l=3$ ($J=\frac{7}{2}$; $T=\frac{1}{2}$ and $T=\frac{3}{2}$) lies within the excitation energy range of the present study ($\sim$10 MeV in ^{31}P), while the preponderance of $l=1$ ($J=\frac{3}{2}$; $T=\frac{3}{2}$), $l=1$ ($J=\frac{1}{2}$; $T=\frac{1}{2}$ and $T=\frac{3}{2}$) and $l=3$ ($J=\frac{5}{2}$; $T=\frac{1}{2}$ and $\frac{3}{2}$) lies at higher excitation energies. The spectroscopic factors extracted for positive-parity states indicate that the currently definitive shell-model calculations for *sd*-shell nuclei correctly predict the essential features of $2s_{1/2}$ and $1d_{3/2}$ dynamics in the Si–P region but probably predict too little vacancy in the lowest-lying $1d_{5/2}$ orbit.

ACKNOWLEDGMENTS

The authors are grateful to Dr. S. Fortier and Dr. S. Galès for many helpful discussions during the course of this work. They are also indebted to R. Marquette and D. Snajzderman for the silicon target preparation. They acknowledge the operating crew of the Orsay M. P. Tandem for the efficient running of the accelerator. This work was supported in part by the U.S. National Science Foundation.

*Present address: University of Tizi Ouzou, Tizi Ouzou, Algeria.

[1]A. C. Wolff and H. G. Leighton, Nucl. Phys. **A140**, 319 (1970).
[2]R. A. Morrison, Nucl. Phys. **A140**, 97 (1970).
[3]H. F. Lutz, D. W. Heikkinen, W. Bartolini, and T. H. Curtis, Phys. Rev. C **2**, 981 (1970).
[4]R. A. McCulloch, N. M. Clarke, R. J. Griffiths, J. S. Hanspal, S. Roman, and J. M. Barnwell, Nucl. Phys. **A431**, 344 (1984).
[5]J. Uzureau, A. Adam, O. Bersillon, and S. Joly, Nucl. Phys. **A267**, 217 (1976).
[6]J. B. French and M. H. Macfarlane, Nucl. Phys. **26**, 168 (1961).
[7]D. A. Outlaw, G. E. Mitchell, and E. G. Bilpuch, Nucl. Phys. **A269**, 99 (1976).
[8]J. Vernotte, G. Berrier-Ronsin, J. Kalifa, and R. Tamisier, Nucl. Phys. **A390**, 285 (1982).
[9]R. G. Markham and R. G. H. Robertson, Nucl. Instrum. Methods **129**, 131 (1975).
[10]P. Picot, Université Paris-Sud, Orsay Internal Report IPNO-

T-81-03, 1981.
[11]J. R. Comfort, Argonne National Laboratory Physics Division Informal Report Phy-1970 B, 1970.
[12]P. M. Endt and C. Van der Leun, Nucl. Phys. **A310**, 1 (1978).
[13]J. Kalifa, J. Vernotte, Y. Deschamps, F. Pougheon, G. Rotbard, M. Vergnes, and B. H. Wildenthal, Phys. Rev. C **17**, 1961 (1978).
[14]P. D. Kunz, private communication.
[15]R. H. Bassel, Phys. Rev. **149**, 791 (1966).
[16]W. W. Daehnick, J. D. Childs, and Z. Vrcelj, Phys. Rev. C **21**, 2253 (1980).
[17]C. M. Vincent and H. T. Fortune, Phys. Rev. C **2**, 782 (1970).
[18]J. Uzureau, A. Adam, O. Bersillon, and S. Joly, Nucl. Phys. **A267**, 245 (1976).
[19]W. W. Dykoski and D. Dehnard, Phys. Rev. C **13**, 80 (1976).
[20]J. Vernotte (unpublished).
[21]M. N. I. Al-Jadir, H. T. Fortune, and D. J. Pullen, J. Phys. G **6**, 731 (1980).
[22]G. T. Kaschl, G. Mairle, U. Schmidt-Rohr, G. J. Wagner, and P. Turek, Nucl. Phys. **A136**, 286 (1969).
[23]H. Mackh, G. Mairle, and G. J. Wagner, Z. Phys. **269**, 353 (1974).
[24]B. H. Wildenthal and P. W. M. Glaudemans, Nucl. Phys. **A108**, 49 (1968).
[25]G. A. Hokken, J. A. J. Hermans, and A. van Ginkel, Nucl. Phys. **A211**, 405 (1973).
[26]M. Betigeri, R. Bock, H. H. Duhm, S. Martin, and R. Stock, Z. Naturforsch. **21a**, 980 (1966).
[27]C. Broude, L. L. Green, and J. C. Willmott, Proc. Phys. Soc. London **72**, 1097 (1968).
[28]J. H. Hough, Z. B. du Toit, and W. L. Mouton, Nucl. Phys. **A109**, 393 (1968).
[29]B. M. Paine and D. G. Sargood, Nucl. Phys. **A331**, 389 (1979).
[30]P. M. Endt, At. Data Nucl. Data Tables **23**, 4 (1979).
[31]P. B. Smith and P. M. Endt, Phys. Rev. **110**, 397 (1958).